IN SITU TIME-RESOLVED SYNCHROTRON DIFFRACTION STUDIES OF HIGH TEMPERATURE BAYER DIGESTION

Loan, M[1*], Loughlin, B[2], Haines, J[2], Croker, D[1], Fennell, M[2], Hodnett, BK[1]
[1] *Materials and Surface Science Institute, University of Limerick, Limerick, Ireland*
[2] *Aughinish Alumina, Aughinish Island, Askeaton, Limerick, Ireland*

Abstract

The more extreme conditions and short residence time of the high temperature Bayer digestion stage makes a clear description of digestion chemistry and kinetics difficult. *In situ* time-resolved diffraction using a synchrotron source is well documented for studying hydrothermal dissolution and crystallization mechanisms. This provides a unique method for elucidating digestion chemistry and kinetics, which is possible as the significantly higher photon energy and flux permits X-ray's to penetrate appropriately designed autoclaves. However, currently available apparatus at synchrotron facilities (globally) were unable to cope with the temperature/pressure, corrosive liquor or requirements of dual reagent feed, as found in Bayer digestion. We have developed and used a pressure vessel that models high temperature Bayer digestion; this investigation has been driven by a desire to improve process efficiency and intensity. The 'inconel' pressure vessel has a very thin-walled base permitting the transmission of photons through the vessel and solution contents. Scattered X-rays collected as a function of time from the growing or dissolving crystals provided kinetic data followed from the inception of reagent mixing. Without a high energy X-ray synchrotron source this would otherwise be impossible.

1 Introduction

The role of digestion in the Bayer process is to dissolve the aluminium containing minerals in bauxite, which allows for separation of insoluble phases. Depending on the mineralogy, differing conditions of temperature (and autogenous pressure) are necessary. For example, bauxites higher in boehmite (γ-AlOOH) require more aggressive conditions (250°C) than those rich in gibbsite ($Al(OH)_3$). Higher temperature digestion also dissolves silica, and some iron and titanium, which react to form a variety of insoluble solids. These reactions can consume valuable alumina, soda, or produce variance in alumina inorganic impurity levels. Generally, calcium, in the form of lime ($Ca(OH)_2$), is added during these reactions for one reason or another (Whittington, 1996a, Malts, 1992, Solymar and Zoldi, 1992).

Considerable progress has been made in understanding lower temperature Bayer lime reactions (Rosenberg and Armstrong, 2005). Lime is very unstable (reactive) in Bayer liquors; even at lower temperatures the reaction rate is in the order of minutes. Depending on the solution conditions (temperature, caustic, aluminate and carbonate concentrations), lime will transform to a complex range of layered double hydroxides (in the nominal form of hydrocalumite – $[Ca_2Al(OH)_6]_2$•½CO_2•OH•5½H_2O), tricalcium aluminate ($Ca_3Al_2(OH)_{12}$) or calcite ($CaCO_3$). In lower temperature processes, calcite is more stable and soluble than lime or tricalcium aluminate (at lower caustic and higher carbonate concentrations), but can revert to hydrocalumite at significantly lower than process temperatures (Rosenberg and Armstrong, 2005, Rosenberg et al., 2001, Buttery et al., 2002). Calcite stability increases with temperature (Whittington, 1996a, Whittington and Cardile, 1996). Similar detailed higher temperature studies of lime chemistry are currently unavailable as experimental conditions are more challenging (i.e. temperature/pressure and short residence time). Data relating to causticisation is, however, available (Whittington, 1996a and refs therein), but it is important to consider that tricalcium aluminate is a 'silica free' hydrogarnet ($Ca_3[Fex,Al_{2-x}][(Ti_y,Si1_{-y})O_4]n(OH)_{12-4n}$), and that hydrogarnets can also be iron- or titanium-substituted.

In situ time-resolved diffraction is commonly used for the study of hydrothermal dissolution and crystallization mechanisms (Walton and O'Hare, 2000), and it provides a unique method for further elucidation of high temperature digestion lime chemistry and kinetics. There were, however, a few hurdles to overcome prior to achieving the goal of following (from seconds to minutes) digestion dissolution and crystallization reactions at the inception of reagent mixing.

2 *In situ* time-resolved synchrotron diffraction

The current state of *in situ* time-resolved diffraction has been reviewed by Walton and O'Hare (2000), which we have drawn on for this discussion. Simply, synchrotron-generated X-rays are of significantly higher flux (up to 10 orders of magnitude higher than in the laboratory) and of a wide energy range (10–120 keV). The distribution of flux (number of photons) with respect to energy (wavelength) varies depending on the synchrotron facility used, but generally high flux can be obtained at short wavelengths (i.e. higher energies). This permits *in situ* studies, as a higher energy incident beam will be less absorbed (attenuated) when penetrating sample containers, and a higher flux will increase detection (i.e. reduce data collection times).

Synchrotron experiments using monochromatic X-rays (angle-dispersive), considered identical to any laboratory diffractometer, allows patterns to be recorded in a fraction of what laboratory based studies would take (i.e. followed in milliseconds). To date most *in situ* time-resolved work has concentrated on solid-gas, solid-solid and slurry (very low liquid ratios) reactions, as experimental operation has been restricted to using capillaries (glass or steel) heated by a hot airflow. These systems, pioneered by Norby et al (2000) and refs therein., were very successful, achieving temperatures of 250°C and an applied pressure of 42 bar. However, the use of capillaries (~1 mm ID) restricts applications to 'real' systems.

Although a specific X-ray wavelength for any given synchrotron diffraction experiment can be selected using a monochromator, experiments can also be performed in the energy dispersive mode, utilizing all the incident polychromatic flux. In energy-dispersive X-ray diffraction (EDXRD) the intensities of scattered X-rays are measured by fixed-angle solid-state photon counting and energy discriminating detectors – each Bragg reflection is characterized by an energy dependent on the angle of the detector. To relate the energy of a diffracted beam to the d_{hkl} spacing responsible, Bragg's Law (Equation 1) can be re-arranged using the Planck-Einstein equation (Equation 2) to convert the wavelength of a photon, λ (Angstroms), to energy, E (keV), shown in Equation 3. Equation 3 shows that the energy (E) of a diffracted beam arising from

a particular sample d_{hkl} spacing is inversely proportional to sin (2θ/2), the sine of half of the 2θ angle of the detector.

$$\lambda = 2\, d_{hkl} \sin\theta \quad (1)$$

$$E = hc / \lambda \quad (2)$$

$$E = 6.19926/(d_{hkl} \sin\theta) \quad (3)$$

In EDXRD the high flux and energies incident on the sample can penetrate larger volume reaction vessels (involving mixing). Having a fixed-angle detector means that only small windows in apparatus are necessary for the passage of X-rays, which permits 'real' systems to be studied. EDXRD has been used for the study of chemical reactions, sometimes down to timescales of 0.3 seconds per diffraction pattern. Common reaction cells are virtually identical to small stainless steel Parr hydrothermal autoclaves, but with walls thinned to (~0.3 mm) to minimize beam attenuation (Walton and O'Hare, 2000). As well as direct observation of the time-scale of reaction, measurements allow the determination of quantitative kinetic data by monitoring the area of a Bragg reflection with time. Such data analysis has enabled rate constants to be determined, and kinetic models for crystallization and dissolution to be proposed since the intensity of a Bragg reflection is directly proportional to the amount of diffracting solid (see supplementary equations section).

Studies applicable to Bayer chemistry have previously been investigated, including gibbsite crystallization (seeded and unseeded) kinetics (Fogg et al., 2000, Loh et al., 2000), layered double hydroxides and zeolites (Walton et al., 2001b, Walton and O'Hare, 2000, Fogg et al., 1998). However, no studies have been carried out under the more aggressive conditions of high temperature digestion.

Although initial time-resolved EDXRD studies were in glass and polymer cells at lower temperatures, gradual improvements via material changes (to stainless steel) permitted hydrothermal reactions to be studied – obviously steel attenuates the beam more significantly than polymers or glass. Current cell designs are limited to reactions occurring at around 220°C, due to pressure ratings and stability of the Teflon liner used to protect cell walls (Walton and O'Hare, 2000). Thicker walled cells can, however, be used for studies at higher temperatures/pressures around 330°C by using higher energy/flux sources such as at the Advanced Photon Source (USA), which has around 10 times greater flux (Shaw et al., 2000).

Acceptable spectra (i.e. intensity versus collection time), beyond the beam characteristics (i.e. energy/flux), depend on the vessel wall thickness, vessel material, and the volume and scattering characteristics of the sample positioned in the beam; there should also be no materials or devices blocking the transmission of beam through the vessel arrangement (Walton and O'Hare, 2000). The external diameter (i.e. volume) of the vessel is limiting, as larger vessel volumes require thicker walls to maintain pressure ratings. Although the above requirements can be generally achieved, it has proved difficult to study hydrothermal reactions at the reaction temperature/pressure without involving a period of heat-up. This is most critical to continuous high temperature/pressure processes (i.e. Bayer digestion) and certain hydrothermal reaction systems, as during the heat-up stage alternate phases may precipitate. Systems have been created to mix liquid-liquid reagent streams, under pressure (Graham and Hennessy, 2003), or under non-hydrothermal conditions (Quayle et al., 2002, Alison et al., 2003) where steam generation is insignificant. Obviously, generation of steam adds complication, as do slurries, where transfer becomes more complicated.

3 Experimental

3.1 *Time-resolved synchrotron diffraction experiments*

All time-resolved experiments were performed at the UK Synchrotron Radiation Source (SRS) CLRC Daresbury. The low emittance SRS storage ring operates with an electron beam energy of 2 GeV and a ring current of 180–250 mA. Station 16.4 (http://srs.dl.ac.uk/XRD/16.4/) was used for these studies. Samples were irradiated with the polychromatic beam produced by 6 T wiggler magnets, and the diffracted beams passed through three 100 μm gap collimators at different 2θ angles, prior to falling on 3 solid state detectors set at slightly different angles. These detectors collect the diffracted beams (according to their energies) into 4000 channels (or bins) over an energy range up to about 120 keV. The energy distribution on station 16.4 has a useful range of 20–70 keV and a peak of intensity around 40–50 keV. The detector angles were adjusted to make the diffracted beams correspond to d spacing energies in the range 20–70 keV. The three detectors were separated by about 2.8° in 2θ. A suspension of anatase was used to calibrate the detectors in 2θ and energy.

3.2 *The new apparatus and experimental operation*

The use of current *in situ* synchrotron diffraction systems (globally), which involve heating up reagents to temperature (Walton and O'Hare, 2000), would result in the crystallization of different phases through the reaction of lime with aluminate liquors (i.e. hydrogarnets and tricalcium aluminate). This is why, for example, in many Bayer digestion studies lime is physically separated (i.e. in a thimble) from the liquor inside a Parr hydrothermal cell, and then subsequently mixed at temperature. Beyond the mixing/heating constraints, the currently used stainless steel vessels at station 16.4 were also unable to cope with the reaction temperature/pressure (250°C and 50 bar) and the corrosive nature of Bayer liquors.

To overcome this we assembled an experimental apparatus to follow the dissolution and crystallization mechanisms from the inception of reagent mixing at 250°C (Figure 1). This is the first example of such an arrangement for *in situ* studies at more extreme reaction conditions (temperature, pressure and corrosive liquors). The new apparatus, based on previous experience at station 16.4 contains two separate (top and bottom) pressure vessel components to permit reagent mixing. The top vessel houses the liquor at temperature, and the bottom vessel contains the solids where crystallization and dissolution occurs in the path of the beam after the mixing of liquor and solids.

An alloy well known to the Bayer industry, inconel, was chosen as it has a tensile strength around 2 times that of stainless steel and high resistance to caustic, having negligible corrosion rates. This permits the walls of the vessel in the path of the beam to be thinned to levels lower than current stainless steel vessels. Inconel wall thickness calculations were based on the volume of the vessel (maximum working pressure), properties of the material (tensile strength) and beam attenuation. Having approximately 25% more nickel than steel, beam attenuation is more significant than in stainless steel, which was measured for our vessels to determine the appropriate wall-thickness.

Unlike that occurring industrially, a batch process was used, as continuous design would have been far more complicated. However, batch operation was not as straightforward as first expected. For example, due to the low liquor volumes head pressures in both vessels were necessary to prevent excessive steam generation (i.e. concentration of liquor) on heat-up and transfer of liquor to the bottom vessel. To counter act this the concentration of liquor added in the top vessel was adjusted. Steam generation could also be reduced by transferring liquor using a gravity feed arrangement (instead of pressure differential), and by using appropriate tubing and valve arrangements (see Figure 1). The most appropriate vessel arrangement also involved the liquid added using an angled inlet tube (Figure 1).

Experimental operation involved placing the solids (anatase, lime, sodalite or bohemite) in the bottom vessel and sodium aluminate liquor in the top vessel (anatase was sourced from Sigma-aldrich chemicals, with lime, sodalite, Bayer liquor and bohemite supplied by Aughinish Alumina). Both vessels were heated to temperature (i.e. 250°C), but with the bottom vessel having a slight bias. This was to compensate for temperature loss on transfer of 20 ml of liquor from the top vessel through the slightly cooler valve separating the two vessels (Figure 1). A head pressure was added to the top vessel (at ambient temperature) using nitrogen to produce a final pressure (at temperature) slightly higher than steam table values. A gas charge of nitrogen was also added to the bottom vessel (but at temperature) where appropriate to reduce steam generation on transfer of liquor from the top vessel using gravity feed. With both vessels at 250°C, the synchrotron beam and detectors were turned on, and the contents of the top vessel transferred to the bottom vessel via opening remotely controlled solenoid and pneumatic valves. In the bottom vessel, stirring occurred via a magnetic flea rotated by a

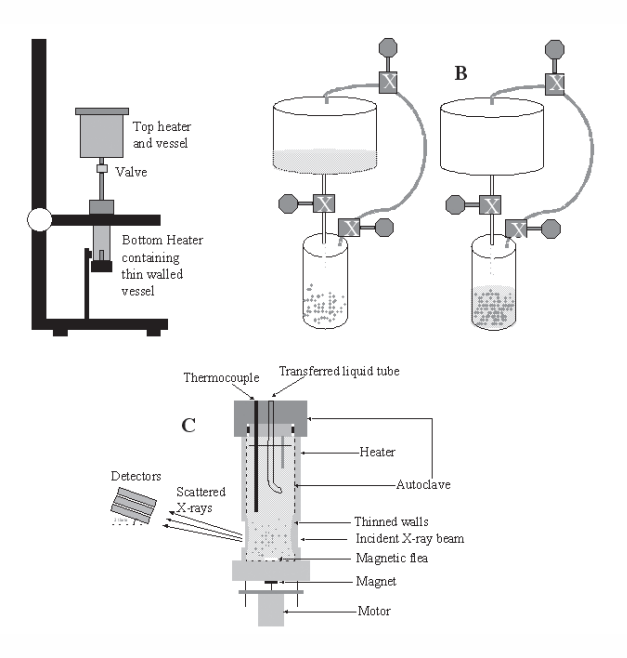

Figure 1: Very simplified schematics of the autoclaves used for studying high temperature Bayer digestion using in situ time resolved synchrotron diffraction. The vessels used involve a complicated assembly that has not been shown. (A) Side profile (in direction of beam) showing the top and bottom vessels separated by a valve in a framework which has x, y and z movement. (B) Simplified representation of liquor transfer at temperature to the bottom vessel containing the solids, which can be performed by gravity feed or via pressure differential using multiple valves. (C) Bottom vessel arrangement (perpendicular to beam), where the heater contains cut out windows to allow the transmission of beam, and the autoclave with thinned walls to reduce beam attenuation.

magnet attached to a motor outside the vessel (see Figure 1). Control and monitoring of the autoclave and the collection of diffraction data from dissolution and crystallization reactions all occurred remotely.

4 *In situ* time-resolved synchrotron diffraction of high temperature digestion reactions

4.1 *Bohemite and anatase*

Anatase (TiO_2) retards the dissolution of aluminium containing minerals (Prakash and Horvath, 1979, Malts, 1992). Rutile is also known to retard dissolution, but its action is slower and shows little impact during the short residence time of digestion. It has been postulated that anatase dissolution results in re-precipitation of a fine fibrous sodium titanate ($Na_xTi_yO_z$•(OH)) phase that forms an impervious surface coating on bauxite minerals (Malts, 1992). Under the higher temperature conditions used to dissolve bohemite, goethite (α-FeOOH) and alumogoethite ($(Fe_{1-x},Al_x)OOH$) can transform to hematite (α-Fe2O3) (Malts et al., 1985, Suss and Maltz, 1992). The dissolution of goethite and subsequent re-precipitation of hematite is a process limited by available seed (i.e. growth sites), and it is thought that a sodium titanate coating also gives rise to colloidal iron formation, and thus generates iron in hydrate (Basu, 1983, Basu et al., 1986, Fulford, 1989).

The dissolution of bohemite (0.5 g) was investigated at 250°C in spent liquor (A/C = 0.35, A = 85 as gL^{-1} Al_2O_3, C = 245 as gL^{-1} Na_2CO_3 and 26 gL^{-1} Na_2CO_3), both with and without anatase (0.5 g). Aughinish Alumina spent liquor was used, as anatase in synthetic liquor does not inhibit bohemite dissolution, possibly due to Bayer organics stabilising the sodium titanate layer. Figure 2A shows the rapid dissolution of bohemite at 250°C in spent liquor. However, in the presence of anatase as shown in Figure 2B, the rate of bohemite dissolution is significantly reduced.

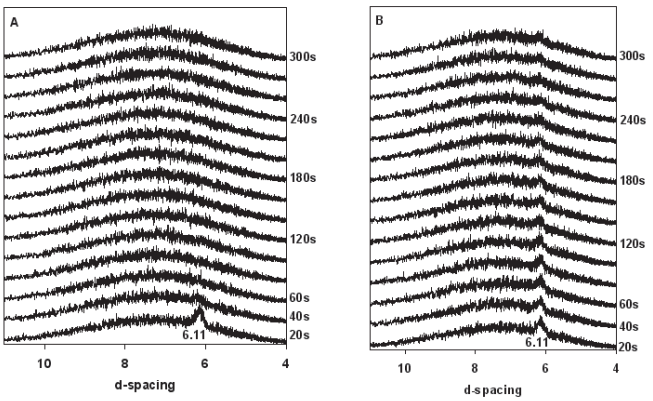

Figure 2: (A) In situ time-resolved synchrotron diffraction patterns demonstrating the rapid dissolution of bohemite in spent liquor at 250°C via the disappearance of the main bohemite (020) reflection at 6.11 Å. (B) In situ time-resolved synchrotron diffraction patterns demonstrating the inhibition of bohemite dissolution in spent liquor at 250°C by anatase. The main bohemite (020) reflection is at a d spacing of 6.11 Å. The (101) anatase reflection at 3.52 Å is not shown but remained throughout the time-resolved patterns.

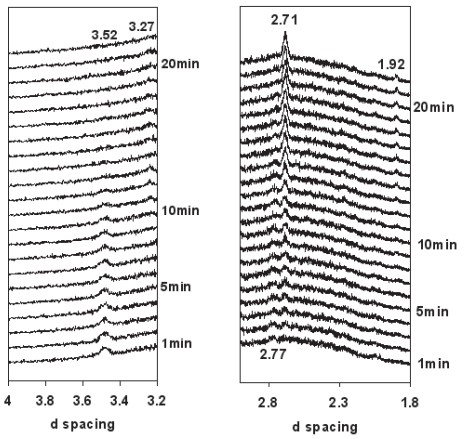

Figure 3: *In situ* time-resolved synchrotron diffraction patterns of the reaction between lime (portlandite) and anatase (TiO_2) in synthetic Bayer liquor at 250°C to form calcium titanate (perovskite). No lime reflections (e.g. (101) at 2.62 Å) were observed in this experiment. The kinetics of perovskite ($CaTiO_3$) formation can be followed via the disappearance of the main (101) anatase reflection (3.52 Å) and the increase of the two major perovskite (121) and (040) reflections at 2.71 and 1.92 Å, respectively. The reflection at a 2.77 Å is believed to be that of a Ti-hydrogarnet or tricalcium aluminate.

4.2 *Lime and anatase*

The impact of anatase can be reduced by the addition of lime ($Ca(OH)_2$) to digestion. A coarse and granular calcium titanate ($CaTiO_3$) phase precipitates, nominally as perovskite (Prakash and Horvath, 1979, Malts, 1992). It is thought that this releases iron mineral surfaces to act as seed, reducing colloidal iron formation (Basu et al., 1986), and also permits bohemite dissolution. Titanate reactions are poorly understood, particularly in relation to titanium-containing hydrogarnet ($Ca_3[Fe_x,Al_{2-x}][(Ti_y,Si_{1-y})O_4]n(OH)_{12-4n}$) formation; wet chemical analyses of Aughinish Alumina samples suggest substitutions of around 0.5–1% TiO_2 and 0.2–0.4% Fe_2O_3 on a mud basis. Hydrogarnet formation also restricts further process optimisation with respect to its higher consumption of lime than titanates. Although evidence suggests that the CaO: TiO_2 ratio is the most important parameter, relevant studies provide conflicting observations regarding the conditions (temperature, caustic, residence time) which favour the formation of a metastable calcium hydroxytitanate (hydrocassite/cassite – $CaTi_2O_4(OH)_2$), perovskite, or hydrogarnets of variable substitution (Rudashevskii et al., 1977, Solymar and Zoldi, 1992, Solymar et al., 1989, Suss and Maltz, 1992, Prakash and Horvath, 1979, Malts et al., 1985, Malts, 1992, Gu et al., 1989). This suggests reaction kinetics to be significant and in particular the instability of lime in Bayer liquors.

The reaction of lime and anatase (1: 1 CaO: TiO_2 ratio) was investigated at 250°C and in synthetic liquor (A/C = 0.68, A = 130 as gL^{-1} Al_2O_3, C = 190 as gL^{-1} Na_2CO_3 and 20 gL^{-1} Na_2CO_3). Note the absence of silica, which would allow only Ti-hydrogarnets or tricalcium aluminate to form in preference to perovskite. Data from an alternate (barium titanate) and lower temperature system (Walton et al., 2001a) suggested the reaction of anatase was likely to be slower than the rate of lime dissolution (Rosenberg et al., 2001). In our experiments, no evidence of lime was found within the first 20 minutes of reaction using 1 minute collection times (Figure 3). This indeed demonstrates lime dissolution to be very rapid at these temperatures, on the time-scale of seconds.

The time-resolved patterns collected (Figure 3) demonstrate the dissolution of anatase to be significantly slower, delaying the formation of perovskite. We do not believe the relative rates of anatase and lime dissolution to be a function of particle size, as both where fine powders. The rapid formation of the reflection at 2.77 Å is believed to belong to a hydrogarnet phase (i.e. (420) reflection). It appears to decrease with the duration of the experiment. This phase must be silica-free (i.e. tricalcium aluminate) or contain Ti-substitution, which may explain its instability. Although in laboratory Parr bomb tests we have found cassite ($CaTi_2O_4(OH)_2$) to sometimes form, it may have also precipitated during this test as a small reflection at 3.27 Å appears and then disappears in Figure 3. However, formation of all such metastable phases could not be confirmed due to the absence of reflections at higher d spacings (6–4 Å), where the detection limit is reduced. There remains plenty to understand with respect to chemistry in this system.

4.3 *Desilication products (DSP)*

Soluble silica (from kaolin and quartz) reacts to form desilication products (DSP). Metastable sodalite (hydroxysodalite) is the dominant lower temperature phase, with cancrinite being the more thermodynamically stable higher temperature phase. Both can be represented by the generic formula of $Na_6[AlSiO_4]_62NaX•nH_2O$, where X can commonly be ½ CO_3^{2-}, ½ SO_4^{2-}, Cl^-, OH^- and NO_3^- (Riley et al., 1999 and refs therein). In higher temperature processes, residual (after desilication) kaolin and a small amount of quartz will transform directly and rapidly to cancrinite. Sodalite will also transform, but it proceeds at a slower rate (Barnes et al., 1999b, Barnes et al., 1999a, Gerson et al., 1996, Riley et al., 1999, and refs therein). Due to its lower solubility and ability to incorporate structural calcium and carbonate (i.e. a form of causticisation), cancrinite is often the favoured DSP analogue. DSP formation also reduces process efficiency through scaling on heat exchangers prior to gibbsite precipitation (Gerson et al., 1996), but the affect can be reduced by lowering silica concentrations via cancrinite formation. Beyond calcium cancrinite formation, lime addition can also be used to form hydrogarnets (Whittington, 1996b, Whittington and Cardile, 1996, Whittington and Fallows, 1997). Although this reduces soda losses and lowers soluble silica, the consumption of alumina often makes calcium cancrinite formation more desirable.

The rate of calcium cancrinite formation at 250°C from sodalite with lime addition was investigated (A/C = 0.67, A = 134 as gL^{-1} Al_2O_3, C = 200 as gL^{-1} Na_2CO_3 and 25 gL^{-1} Na_2CO_3). The ratio by mass of solids was 7.5: 1 (sodalite: CaO). In the absence of lime the kinetics of transformation were very slow. It should be noted that in these experiments the carbonate concentration, well known to affect this process, was lower than that commonly found in Australian Bayer plants. Again, no lime reflections (e.g. (101) at 2.62 Å) were observed (Figure 4), confirming previous interpretations. In Figure 4, the rate of calcium cancrinite formation from sodalite is demonstrated via the appearance and increase of its unique (211) reflection at 3.21 Å. The (222) and (411) sodalite reflections (2.59 and 2.12 Å) also show some degree of broadening and relative reduction in intensity. However, the (110) and (211) sodalite reflections (6.33 and 3.67 Å) show little change. There is also some evidence of the (101) cancrinite reflection at 4.60 Å. The reflection at 2.73 could be attributed to a hydrogarnet or cancrinite. Although this data shows a delay, or induction time in transformation kinetics we believe this is more a function of the initially 'silica-free' synthetic liquor, as sodalite has to first dissolve and reach saturation, unlike the case in Bayer plants.

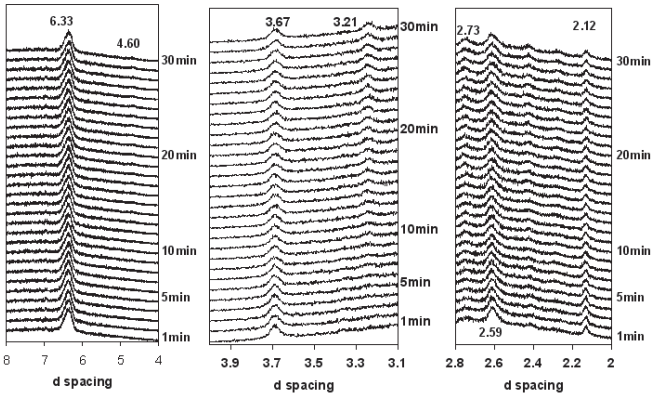

Figure 4: *In situ* time-resolved synchrotron diffraction patterns of the transformation of sodalite to calcium cancrinite through the addition of lime. No lime reflections (e.g. (101) at 2.62 Å) were observed in this experiment. The kinetics calcium cancrinite formation can be followed via the appearance and increase of its unique (211) reflection at 3.21 Å. The (222) and (411) sodalite reflections (2.59 and 2.12 Å) also show some degree of broadening and relative reduction. However, the (110) and (211) sodalite reflections (6.33 and 3.67 Å) show little change. There is also some evidence of the (101) cancrinite reflection at 4.60 Å. The reflection at 2.73 could be attributed to a hydrogarnet or cancrinite.

5 Conclusions

A new technique for studying high temperature Bayer digestion reactions has been documented through the development of a novel pressure vessel apparatus. *In situ* time-resolved synchrotron diffraction of digestion reactions at 250°C using this apparatus has provided further kinetic information, particularly with respect to the reactivity of lime. Although quantitative kinetic determinations could be made (see supplementary equations section), due to the infancy of this technique, we have decided to be more cautious regarding the data developed for the dissolution and inhibition of bohemite, and the formation of perovskite and calcium cancrinite.

Acknowledgements

We thoroughly thank Dr DJ Taylor and A Neild at the Daresbury laboratory who spent considerable time helping us develop the pressure vessels for usage at station 16.4. SRS CLRC Daresbury laboratory and the European Union are thanked for access to the synchrotron facilities at Daresbury through the European Community-Research Infrastructure Action under the FP6 'Structuring the European Research Area' Programme award (number 42187). Dr Louise Clune, Audrey Ryan, Doireann Boyle and Dr Donncha Haverty are thanked for their assistance with performing the experiments at Daresbury. Baskerville Autoclaves (Manchester UK) are thanked for their construction and design support with the autoclaves. Enterprise Ireland (Irish government) and Aughinish Alumina are thanked for their financial support of this work through an Innovation grant number IP-2004-0191.

Supplementary Equations

Integrated peak area data is often converted into the dimensionless quantity termed the extent of reaction (α). The value of α at any time (t) for the growth of a crystalline phase is defined by Equation 4:

$$\alpha_{hkl}(t) = I_{hkl}(t) / I_{hkl}(t_{\infty}) \quad (4)$$

where $I_{hkl}(t)$ represents the integrated peak area of a reflection (hkl) at time t, and $I_{hkl}(t_{\infty})$ represents the integrated peak area of a reflection (hkl) when the reaction is complete. The dissolution (or decay) of a crystalline phase can be represented in a similar manner (Equation 5):

$$\alpha_{hkl}(t)_{\text{dissolution}} = 1 - [I_{hkl}(t) / I_{hkl}(t_0)] \quad (5)$$

where $I_{hkl}(t_0)$ represents the initial integrated peak area of that reflection (hkl). Least-squares fits of the $\alpha_{hkl}(t)$ data to kinetic models in the general form of the Avrami-Erofe'ev equation have been successfully applied in similar systems to extract mechanistic kinetic data and rate constants (Walton et al., 2001a).

References

Alison, H. G., Davey, R. J., Garside, J., Quayle, M. J., Tiddy, G. J. T., Clarke, D. T. and Jones, G. R. (2003) Physical Chemistry Chemical Physics, 5, pp. 4998–5000.
Barnes, M. C., Addai-Mensah, J. and Gerson, A. R. (1999a) Colloids and Surfaces a-Physicochemical and Engineering Aspects, 147, pp. 283–295.
Barnes, M. C., Addai-Mensah, J. and Gerson, A. R. (1999b) Microporous and Mesoporous Materials, 31, pp. 287–302.
Basu, P. (1983). Light metals 1983 (ed E. M. Adkins), TMS, pp. 83–97.
Basu, P., Nitowski, A. and The, P. (1986) In Iron Control in Hydrometallurgy (Ed, A. J. Monhemius and J.E. Dutrizac) Ellis Horwood, pp. 222–244.
Buttery, J. H. N., Patrick, V. A., Rosenberg, S. P., Heath, C. A. and Wilson, D. J. (2002) In Light Metals 2002 (Ed, Schneider, W.) TMS, pp. 185–190.
Fogg, A. M., Dunn, J. S., Shyu, S. G., Cary, D. R. and O'Hare, D. (1998) Chemistry of Materials, 10, pp. 351–355.
Fogg, A. M., Price, S. J., Francis, R. J., O'Brien, S. and O'Hare, D. (2000) Journal of Materials Chemistry, 10, pp. 2355–2357.
Fulford, G. (1989) Light Metals 1989, pp. 77–89.
Gerson, A. R., Addai-Mensah, J., Zheng, K., O'Dea, A. and St.C., S. R. (1996) In Fourth International Alumina Quality Workshop, Darwin, pp. 393.
Graham, G. M. and Hennessy, A. J. B. (2003) In Chemistry in the Oil Industry VIII, Biddles Ltd, Manchester, pp. 141–153.
Gu, S., Cao, R. and Chen, X. (1989) Rare Met., 8, pp. 14–18.
Loh, J. S. C., Fogg, A. M., Watling, H. R., Parkinson, G. M. and O'Hare, D. (2000) Physical Chemistry Chemical Physics, 2, pp. 3597–3604.
Malts, N. (1992) Light Metals 1992, TMS, pp. 1337–1342.
Malts, N., Poddymov, V., Rudashevskii, L. and Kiselev, V. (1985) Tsvetnye Metally / Non Ferrous metals, 11, pp. 40–43.
Norby, P., Hanson, J. C., Fitch, A. N., Vaughan, G., Flaks, L. and Gualtieri, A. (2000) Chemistry of Materials, 12, pp. 1473–1479.
Prakash, S. and Horvath, Z. (1979) Publ. Tech. Univ. Heavy Ind., Ser. B, 34, pp. 43–63
Quayle, M. J., Davey, R. J., McDermott, A. J., Tiddy, G. J. T., Clarke, D. T. and Jones, G. R. (2002) Physical Chemistry Chemical Physics, 4, pp. 416–418.
Riley, G., Smith, P., Binet, D. and Pennifold, R. (1999) In Fifth International Alumina Quality Workshop, Bunbury 21–26, pp. 404–414.
Rosenberg, S. P. and Armstrong, L. (2005) In Light Metals 2005 (Ed, Kvande, H.), TMS, pp. 157–161.
Rosenberg, S. P., Wilson, D. J. and Heath, C. A. (2001) Light Metals 2001, pp. 19–25.

Rudashevskii, L., Malts, N., Firfarova, I. and Neroslavskii, L. (1977) Izv. Akad. Nauk SSSR Met., 6, pp. 79–82.
Shaw, S., Clark, S. M. and Henderson, C. M. B. (2000) Chemical Geology, 167, pp. 129–140.
Solymar, K. and Zoldi, J. (1992), Light Metals 1992, TMS, pp.185–193.
Solymar, K., Zoldi, J. and Ferenczi, T. (1989) Magy. Alum., 26, pp. 20–29.
Suss, A. and Maltz, N. (1992) Light Metals 1992, TMS, pp. 1343–1347.
Walton, R. I., Millange, F., Smith, R. I., Hansen, T. C. and O'Hare, D. (2001a) Journal of the American Chemical Society, 123, pp. 12547–12555.
Walton, R. I. and O'Hare, D. (2000) Chemical Communications, pp. 2283–2291.
Walton, R. I., Smith, R. I. and O'Hare, D. (2001b) Microporous and Mesoporous Materials, 48, pp. 79–88.
Whittington, B. and Fallows, T. (1997) Hydrometallurgy, 45, pp. 289–303.
Whittington, B. I. (1996a) Hydrometallurgy, 43, 13–35.
Whittington, B. I. (1996b) In Fourth International Alumina Quality workshop, Darwin, pp. 413–424.
Whittington, B. I. and Cardile, C. M. (1996) International Journal of Mineral Processing, 48, pp. 21–38.